Journal of Molecular Structure 1205 (2020) 127622

Contents lists available at ScienceDirect

Journal of Molecular Structure

journal homepage: http://www.elsevier.com/locate/molstruc

2-Halo- and/or 4-ethoxycarbonyl-substituted asymmetric 1,3-diaryltriazenes and 1,3-diarylamidines as well as *N*-methylated congeners

Silvio Preusser [a, 1], Paul R.W. Schönherr [a], Helmar Görls [a], Sven Krieck [a], Wolfgang Imhof [b], Matthias Westerhausen [a, *]

[a] Institute of Inorganic and Analytical Chemistry, Friedrich Schiller University, Humboldtstraße 8, 07743, Jena, Germany
[b] Institute for Integrated Natural Sciences, Department of Chemistry, University Koblenz-Landau, Universitätsstraße 1, D-56070, Koblenz, Germany

ARTICLE INFO

Article history:
Received 8 October 2019
Received in revised form
13 December 2019
Accepted 18 December 2019
Available online 23 December 2019

Keywords:
Diazene
Formamidine
Triazene
Benzotriazole
Hydrogen bridges
E/*Z* isomerism

ABSTRACT

1,3-Diaryltriazenes Ar−N═N−N(R)-R' [R = H; Ar/R' = C_6H_4-4-COOEt/Ph (**1**), C_6H_3-2-Br-4-COOEt/Ph (**2**), CH_2Ph/C_6H_4-4-COOEt (**3**)] and the *N*-methylated congeners [R = Me; Ar/R' = C_6H_4-4-COOEt/Ph (**9**), C_6H_2-2,5-Br_2-4-NH_2/Ph (**10**), C_6H_4-4-Br/C_6H_4-4-COOEt (**11**), C_6H_2-2-Br-4-COOEt/Ph (**12**), C_6H_2-2-Br-4-COOEt-6-Me/C_6H_4-2-Me (**13**), C_6H_3-2-Br-4-F/Ph (**14**), C_6H_3-2-Br-6-F/Ph (**15**), C_6H_3-2-Br-4-Cl/Ph (**16**), C_6H_3-2,4-Br_2/Ph (**17**)] as well as 1,3-diarylformamidines of the type Ar−N═CH−N(R)-R' [R = H; Ar/R' = C_6H_3-4-COOEt/Ph (**4**), C_6H_3-2-Br-4-COOEt/Ph (**5**), C_6H_3-2-Br-4-F/Ph (**6**)] and 1,3-diaryl-3-methylamidines [R = Me; Ar/R' = C_6H_3-4-COOEt/Ph (**18**), C_6H_3-2-Br-4-COOEt/Ph (**19**), C_6H_3-2-Br-4-Cl/Ph (**20**), C_6H_3-2,4-Br_2/Ph (**21**)] crystallize preferably with (*syn*-*E*) configuration. For comparison reasons sterically crowded Ph-N(R)-C(R') = N−C_6H_3-2-Br-4-COOEt [R = H, R' = Ph (**7**), *t*Bu (**8**); R = Me, R' = Ph (**22**), *t*Bu (**23**)] are included. Large substituents destabilize this isomeric form due to intramolecular steric repulsion. 1,3-Diarylformamidines dimerize *via* two nearly parallel N−H···N hydrogen bridges. This kind of aggregation is very beneficial because the N═C−N bond angles are slightly larger than 120°. Narrower N═N−N bond angles are found for the 1,3-diaryltriazenes and therefore, aggregation occurs *via* intermolecular N−H···O hydrogen bridges to O-Lewis bases. The 1,3-diaryl-3-methylformamidines and -triazenes show very similar bonding parameters. Thus, the bond lengths of the N═C/N═N double bonds are approx. 4−9 pm shorter than the N−C/N−N single bonds, supporting charge delocalization within the diazaallyl- and triazaallyl systems regardless of N-methylation.

1. Introduction

Formamidines and triazenes are isoelectronic compounds with a long tradition and very similar properties in many aspects which are widely used and intensively studied according to their widespread applications. Due to their tremendous importance in organic, medicinal and coordination chemistry, diverse aspects of these compound classes have been summarized in numerous excellent reviews (Scheme 1).

Amidines [1] and triazenes [2] are well-known for decades and intensively studied due to the fact that these compounds can easily be prepared [3] and that they provide a plethora of reactivity patterns. The enormous importance of these compound classes is based on early recognized biological and medicinal activity as well as on promising pharmaceutical and clinical applications [4,5]. In organic chemistry, these compounds are widely used for the syntheses of heterocycles [6,7], as nucleophilic catalysts [8], in analytical [9] and as ligands in coordination chemistry [10]. During our studies with respect to the transformation of 1,3-diaryl-3-methyltriazenes into *N*-arylbenzotriazoles for pharmaceutical purposes we became aware of large variation of the yields depending on substitution patterns of the triazenes and reaction conditions. These cyclization reactions have to be mediated by copper or palladium catalysts in the presence of bases (Scheme 2). Depending on the use of *NH*-triazenes (Scheme 2, right) or methylated triazenes (left), the group R′ is bonded at the benzo unit

* Corresponding author.
E-mail address: m.we@uni-jena.de (M. Westerhausen).
URL: http://www.lsac1.uni-jena.de
[1] Present address: S. Preusser Laborchemie Apolda GmbH, Utenbacherstraße 72−74, D-99510, Apolda, Germany.

https://doi.org/10.1016/j.molstruc.2019.127622
0022-2860/

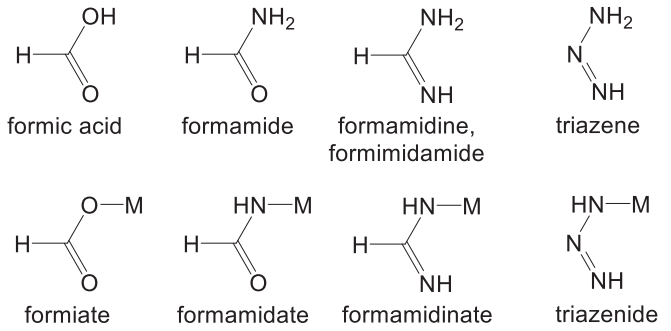

Scheme 1. Isoelectronic rows of the basic compounds (top) and their metalated congeners (bottom) via consecutive replacement of O by NH and finally of CH by N.

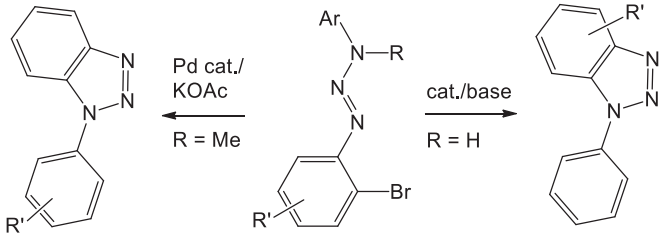

Scheme 2. Catalytic cyclization of 1,3-diaryltriazenes to N-aryl-benzotriazoles via a Buchwald-Hartwig-type cycloamination (R = H, right) or via demethylating cycloamination (R = Me, left).

(Buchwald-Hartwig-type cycloamination) [11] or at the 3-aryl substituent (demethylating cycloamination) [12]. The benchmark reaction of the palladium-mediated synthesis of *N*-4-ethoxycarbonylphenyl-benzotriazole (R' = COOEt) from 1-(2-bromo-4-ethoxycarbonylphenyl)-3-phenyl-3-methyltriazene (Scheme 2, left) showed a strong dependence on the atmosphere (air, oxygen, argon) and on the reaction conditions (excess of base, nature of oxidant and Pd catalyst) [12].

These challenges prompted us to elucidate the influence of the substitution pattern on the molecular structures of 1,3-diaryltriazenes, 1,3-diaryl-3-methyltriazenes, and of 1,3-diarylamidines. 1,3-Diaryltriazenes (E = N) and 1,3-diarylformamidines (E = CH) can adopt different isomeric forms as depicted in Scheme 3. The aryl groups can be positioned at the same (*syn*) or opposite sides (*anti* isomer) of the molecule. Furthermore, *E*/*Z* isomeric forms can be observed at the E = N double bond. However, tautomeric equilibria *via* 1,3-hydrogen migration can interconvert isomeric forms of triazenes and amidines which is well-known [1,2] and will not be discussed here. In addition, the rather acidic N–H functionality (R = H) is prone to the formation of intermolecular hydrogen bridges and hence, the packing of the molecules in the crystalline state should strongly depend on the nature of the *N*-bound group R (hydrogen, methyl).

Due to the fact that we were interested in building blocks for the preparation of pharmazeutically useful *N*-aryl-benzotriazoles we limited our investigation on 1,3-diaryltriazenes, 1,3-diaryl-3-methyltriazenes, and 1,3-diarylamidines with halide functionalities and/or ethoxycarbonyl groups in para-position.

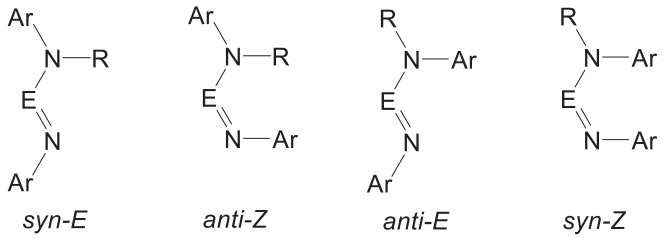

Scheme 3. Differentiation of the isomeric configurations of 1,3-diarylformamidines (E = CH; Ar = aryl) as well as 1,3-diaryltriazenes (E = N; R = H) and 1,3-diaryl-3-methyltriazenes (E = N, R = Me).

2. Experimental

Instrumentation: All reactions were performed under ambient conditions and monitored by TLC on silica with embedded fluorescence indicator. NMR spectra were recorded by the Bruker NMR Spectrometers with 250 MHz, 400 MHz or 600 MHz. Highly resolved masses were obtained by electron spray ionization using a Bruker microTOF-Q by direct injection. The calibration was performed with sodium formiate cluster at the mass range of m/z = 50–1000 Da. Elemental analyses were performed using an EuroVector EuroEA 3000 instrument. Melting points were determined by a Büchi apparatus. IR spectra were record using a Bruker Alpha FT-IR ATR spectrometer. UV spectra were obtained at a Specord UV–Vis spectrometer.

Synthesis: *O*-Ethyl-phenylformimidate was synthesized using a slightly modified procedure of Roberts et al. and purified by fractionized vacuum distillation [13]. The synthesis of *N*-*tert*-butylcarbonyl aniline and *N*-phenylcarbonyl aniline were performed according to a slightly modified procedure according to a literature protocol by mono-*N*-acylation using pivaloyl chloride and benzoyl chloride, respectively [14]. The triazenes were prepared in analogy to well-known published procedures [12]. General procedures for the synthesis of 1,3-diarylformamidines were published earlier [15].

For further details on the synthesis and characterization of these 1,3-diaryltriazenes and 1,3-diarylamidines see the Electronic Supporting Information (ESI).

Crystal structure determinations: The intensity data for the compounds were collected on a Nonius KappaCCD diffractometer using graphite-monochromated Mo-K_α radiation. Data were corrected for Lorentz and polarization effects; absorption was taken into account on a semi-empirical basis using multiple-scans [16–18]. The structures were solved by direct methods (SHELXS) [19] and refined by full-matrix least squares techniques against F_o^2 [20]. The hydrogen atoms of **5**, **7**, and **24** (with the exception of the hydrogen atoms bonded to the amidine nitrogen atom N3) were included at calculated positions with fixed thermal parameters. All other hydrogen atoms were located by difference Fourier synthesis and refined isotropically. The crystal of **5** was a non-merohedral twin. The twin laws were determined by PLATON [21] to (−1.000 0.000 0.000) (−0.368 1.000–0.169) (0.000 0.000–1.000). The contribution of the main component was refined to 0.855 (3). All non-disordered, non-hydrogen atoms were refined anisotropically

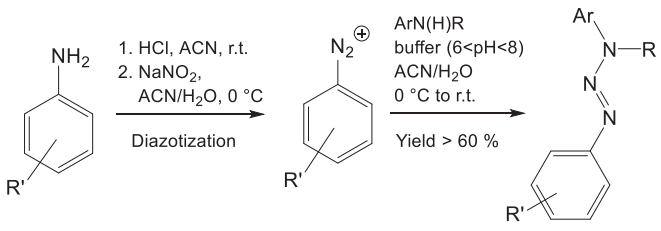

Scheme 4. Synthesis of R-substituted triazenes via diazotization and subsequent reaction with aniline or N-methyl-aniline (ACN acetonitrile, R = H, Me).

Table 1
Substitution patterns and yields of 1,3-diaryltriazenes and 1,3-diaryl-3-methyltriazenes of the type Ar–N=N–N(R)-R' (prepared via diazotization according to Schemes 4 and 6) and of 1,3-diarylamidines and 1,3-diaryl-3-methylamidines (Scheme 8).

	E	R	Ar	R′	Yield (%)[a]	$\delta(^1H_{Me})$	$\delta(^{13}C\{^1H\}_{Me})$
1	N	H	C_6H_4-4-COOEt	Ph	71	–	–
2	N	H	C_6H_3-2-Br-4-COOEt	Ph	70	–	–
3	N	H	CH_2-Ph	C_6H_4-4-COOEt	61	–	–
4	CH	H	C_6H_3-4-COOEt	Ph	37	–	–
5	CH	H	C_6H_3-2-Br-4-COOEt	Ph	43	–	–
6	CH	H	C_6H_3-2-Br-4-F	Ph	66	–	–
7	C-Ph	H	C_6H_3-2-Br-4-COOEt	Ph	56	–	–
8	C-*t*Bu	H	C_6H_3-2-Br-4-COOEt	Ph	50	–	–
9	N	Me	C_6H_4-4-COOEt	Ph	83	3.73	33.3
10	N	Me	C_6H_2-2,5-Br_2-4-NH_2	Ph	69	3.64	32.6
11	N	Me	C_6H_4-4-Br	C_6H_4-4-COOEt	35	3.73	32.3
12	N	Me	C_6H_3-2-Br-4-COOEt	Ph	79	3.77	33.8
13	N	Me	C_6H_2-2-Br-4-COOEt-6-Me	C_6H_4-2-Me	67	3.58	37.7
14	N	Me	C_6H_3-2-Br-4-F	Ph	80	3.70	33.2
15	N	Me	C_6H_3-2-Br-6-F	Ph	76	3.71	32.6
16	N	Me	C_6H_3-2-Br-4-Cl	Ph	78	3.72	33.4
17	N	Me	C_6H_3-2,4-Br_2	Ph	72	3.72	33.5
18	CH	Me	C_6H_3-4-COOEt	Ph	69	3.52	34.5
19	CH	Me	C_6H_3-2-Br-4-COOEt	Ph	79	3.49	34.5
20	CH	Me	C_6H_3-2-Br-4-Cl	Ph	47	3.54	34.5
21	CH	Me	C_6H_3-2,4-Br_2	Ph	60	3.54	34.5
22	C-Ph	Me	C_6H_3-2-Br-4-COOEt	Ph	46	3.53	40.4
23	C-*t*Bu	Me	C_6H_3-2-Br-4-COOEt	Ph	23	2.89	39.1

[a] Yield of isolated crystalline triazenes and amidines.

[20]. The crystal of **7** was extremely thin and of low quality, resulting in a substandard data set; however, the structure is sufficient to show connectivity and geometry despite the high final *R* value. We will only publish the conformation of the molecule and the crystallographic data. We will not deposit the data in the Cambridge Crystallographic Data Centre. Crystallographic data as well as structure solution and refinement details are summarized in Table S1 (see Supporting Information). XP (SIEMENS Analytical X-ray Instruments, Inc.) [22] was used for structure representations.

3. Results and discussion

3.1. Synthesis

Numerous preparative protocols have been developed to prepare symmetrically and asymmetrically substituted amidines [1] and triazenes [2]. Due to the fact that our objective was the synthesis of derivatives of benzotriazoles, we studied mainly asymmetrically aryl-substituted amidines and triazenes with bromo functionalities in *ortho*-position. Another precondition is the tolerance of ester groups in para-position of the aryl substituent during the synthesis of these compounds.

The preferred procedure starts with the diazonium salt of the bromo-substituted aniline which was reacted with aniline, benzylamine or *N*-methyl-aniline according to Scheme 4. During this reaction, pH values of 6–7 (aniline, benzylamine) or 7–8 (*N*-methyl-aniline) have to be maintained in buffered solutions (acetate or carbonate buffers) to suppress side reactions. The pH value is a crucial factor and at low values in acidic media, diaryldiazenes were formed as side products.

This method allowed the synthesis of 1,3-diaryltriazenes and 1,3-diaryl-3-methyltriazenes with generally good yields (Table 1). Halo- and ester groups are tolerated and the yields of isolated crystalline compounds are larger than 60%. During separation and isolation of the 1,3-diaryl-3-methyltriazenes, intensively orange-red side products were occasionally formed with yields below 3% which were chromatographically isolated and recognized as diaryldiazenes Ar'-N=N–C_6H_4-4-NHMe due to an attack of the diazonium salt Ar'-N_2^+ at the para-position of *N*-methyl-arylamine; the X-ray structure determination of the diazene 2-Br-4-EtOOC-6-MeC_6H_2–N=N–C_6H_3-3-Me-4-NHMe (**24**) verified the formation of this side product as shown in Scheme 5.

Molecular structure and atom labeling scheme of the diazene **24** are depicted at the top of Fig. 1. In the solid state, intermolecular hydrogen bridges between the N3–H3 functionality and the ester carbonyl group C8=O1 lead to a strand structure as shown at the bottom of Fig. 1. The N1=N2 bond length of 120.0 (6) pm is a typical double bond value. The N1–C1 and N2-11 distances of 148.7 (6) and 147.9 (7) pm, respectively, are characteristic single bond values with negligible interactions between the diazene and aryl π-systems. Formation of intermolecular N3–$H3_{N3}\cdots O1'$ hydrogen bridges leads to strand formation in the crystalline state.

Diazotization of 1,4-diaminobenzene with two equivalents of sodium nitrite in water and subsequent addition of a solution of

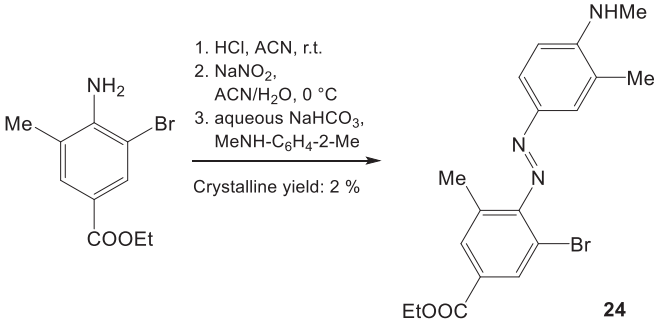

Scheme 5. Isolated side product during diazotization and reaction with N-methyl-2-toluidine yielding the diazene 2-Br-4-EtOOC-6-MeC_6H_2–N=N–C_6H_3-3-Me-4-NHMe (**24**).

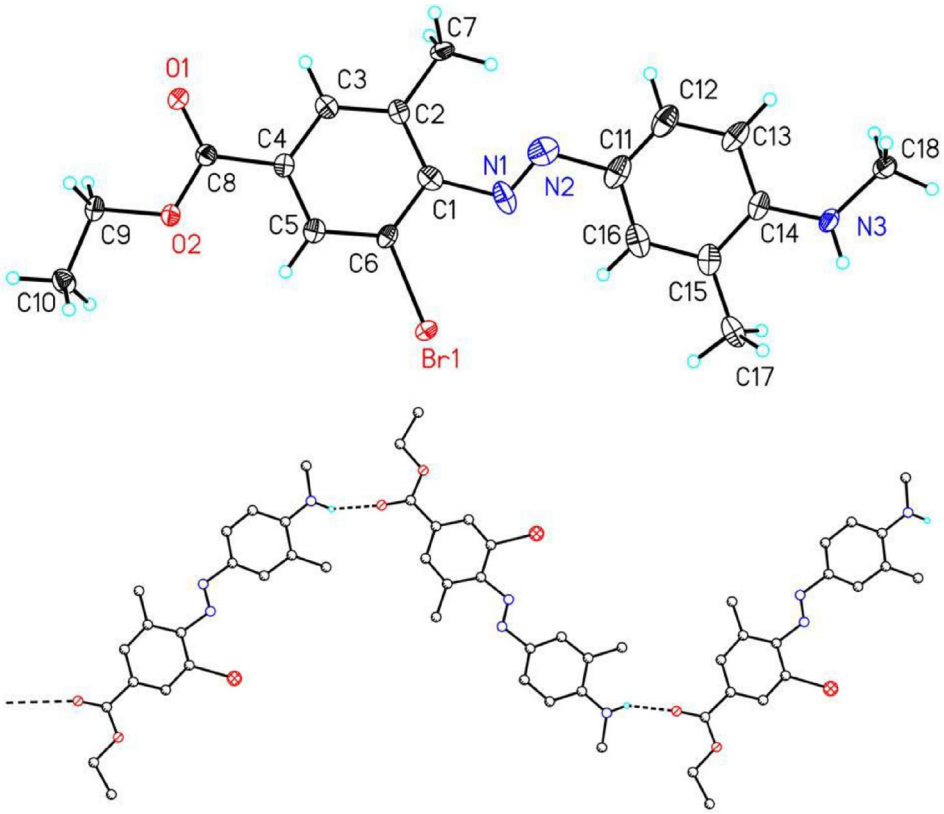

Fig. 1. Molecular structure and labeling scheme of diazene 2-Br-4-EtOOC-6-MeC_6H_2–N=N–C_6H_3-3-Me-4-NHMe (**24**, at the top). The ellipsoids represent a probability of 30%, H atoms are shown with arbitrary radii. At the bottom, aggregation via intermolecular N–H···O hydrogen bridges is depicted; the hydrogen bridges are symbolized by dotted lines. Atoms are shown with arbitrary radii, C-bound hydrogen atoms are omitted for the sake of clarity.

aniline in alcohol yielded 54% of 1,4-bis(3-phenyltriazen-1-yl) benzene [23]. Contrary to this report, 1,4-diamino-2,5-dibromobenzene did not react in a similar manner. 1,4-Diamino-2,5-dibromobenzene was combined with HCl and sodium nitrite in acetonitrile; subsequent addition of *N*-methyl-aniline yielded only the monotriazene congener 1-(2,5-dibromo-4-aminophenyl)-3-methyl-3-phenyltriazene (**10**) as depicted in Scheme 6. The amino group in trans-position to the diazo functionality remained unchanged and doubly bis(triazene) derivatives were not accessible by this protocol regardless of the applied stoichiometry of the substrates.

As an alternative pathway, arylazides can be reacted with phenyllithium, however, the ester functionality was very reactive toward phenyllithium. Two thirds of the substrate remained unchanged, if the precise 1:1 stoichiometry was applied, and one third formed a product which consumed three equivalents of PhLi yielding triazene **25** (Scheme 7). Thus, the yield was 32% with respect to the starting arylazide (yield of 96% with respect to PhLi). This finding showed that the presence of ester functionalities limits the preparative access to asymmetric triazenes with ester substituents and only the beneficial diazotization method (Scheme 5) gave satisfactory yields as depicted in Table 1.

Methylation of 1,3-diaryltriazenes *via* potassiation with KH and subsequent methylation with MeI in THF yielded the methylated products with the methyl groups at one of the nitrogen bases, regiocontrol was challenging and depended on the steric shielding. Hence, the conversion of 1-(4-ethoxycarbonylphenyl)-3-benzyltriazene led to a mixture of 1-(4-ethoxycarbonylphenyl)-3-benzyl-3-methyltriazene, 1-benzyl-3-(4-ethoxycarbonylphenyl)-3-methyltriazene, and (4-ethoxycarbonylphenyl)-benzyl-methylamine, the latter product formed *via* elimination of dinitrogen.

The beneficial preparative procedure for the synthesis of asymmetric 1,3-diarylformamidines consisted of the reaction of the substituted aniline with *N*-phenyl-*O*-ethylimidate at room temperature or 50 °C (Scheme 8, right). The syntheses of 1,3-diaryl-3-methylformamidines succeeded by the reaction of substituted anilines with *N*-methyl-*N*-phenylformamide (Scheme 8, left). The yields are given in Table 1.

3.2. Molecular structures

The molecular structure and atom labeling scheme of (*syn-E*)-$PhCH_2$-N=N–N(H)–C_6H_4-4-COOEt (**3**) are depicted at the top of

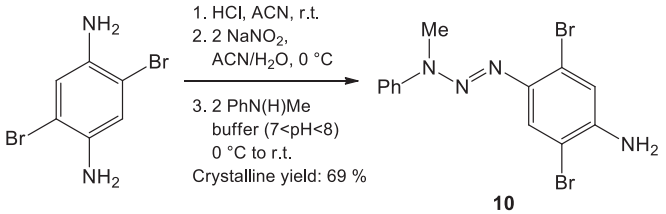

Scheme 6. Reaction of 1,4-diamino-2,5-dibromobenzene with excess of sodium nitrite and N-methyl-aniline yielding 1-(2,5-dibromo-4-aminophenyl)-3-methyl-3-phenyltriazene regardless of the applied stoichiometry of the components.

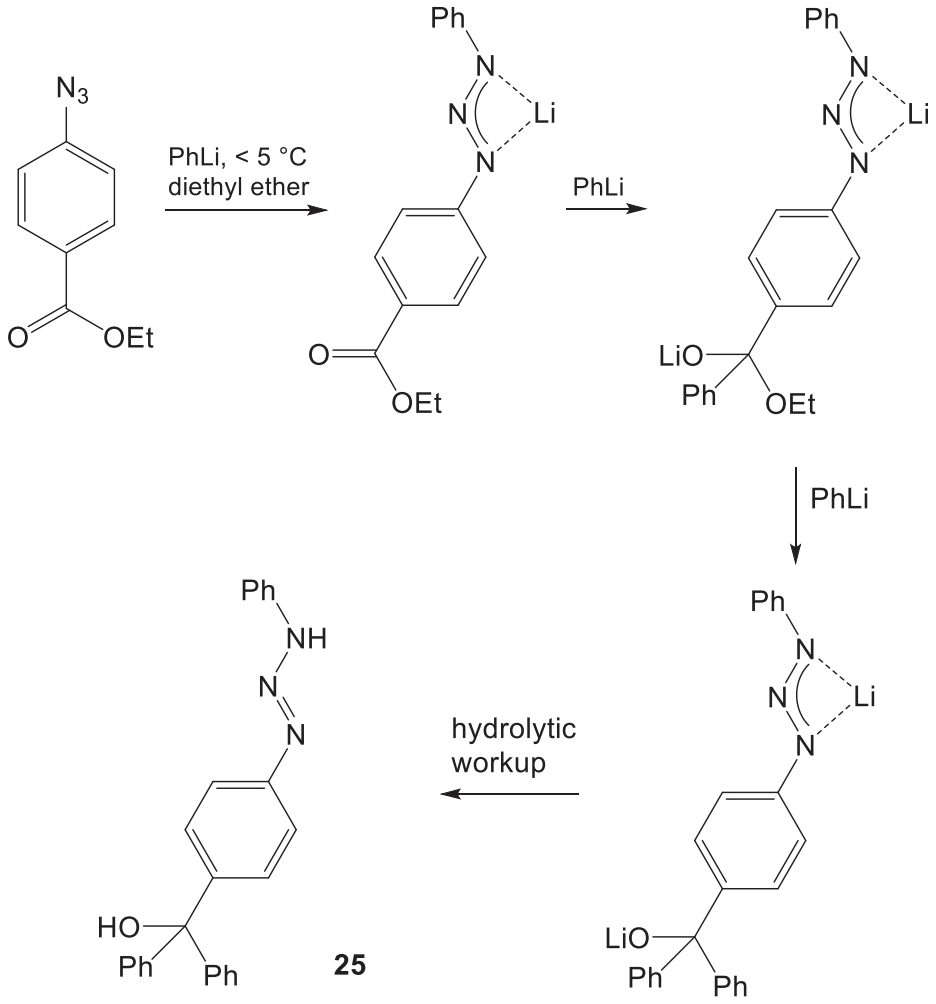

Scheme 7. Stepwise reaction of 4-ethoxycarbonylphenylazide with three equivalents of phenyllithium and subsequent hydrolytic workup yielded 1-[4-(hydroxydiphenylmethyl) phenyl]-3-phenyltriazene (**25**).

Fig. 2. The methylene moiety at N1 prevents an effective interaction of the π-systems of the triazene and benzyl units. This substitution leads to a slight shortening of the N═N bond and a reduction of the NNN bond angle by approx. 2° in comparison to diaryltriazenes (see below). In addition, the interaction of the conjugated π-systems of the N═N–N and aryl moieties leads to a shortening of the N-$C_{R'}$ bond to 139.0 (2) pm. Repulsion between the free electron pair at the middle atom N2 and the C13–H bond leads to different N3–C8–C9 (117.52 (13)°) and N3–C8–C13 (122.64 (13)°) bond angles. In the crystalline state, aggregation occurs *via* intermolecular N3–$H3_{N3}$···O2A hydrogen bridges (N3···O2A 285.7 (2), N3–$H3_{N3}$ 89 (2), O2A···$H3_{N3}$ 200 (2) pm; N3–$H3_{N3}$–O2A 160.2 (18)°) to the carbonyl group (Fig. 2, bottom), leading to the formation of a strand-like structure.

Molecular structure and atom labeling scheme of (*syn-E*)-4-[Ph_2(HO)C–C_6H_4-]N═N–N(H)-Ph (**25**) (top) as well as aggregation in the crystalline state (bottom) are depicted in Fig. 3. The charge delocalization within the triazene unit of **25** is significantly more pronounced than in **1**, expressed by the difference of the N═N and N–N bond lengths (**3**: 9.0 pm, **25**: 3.8 pm). The reason for this increasing convergence is the fact that both nitrogen atoms in 1- and 3-positions of the triazene are involved in the intermolecular hydrogen bridges N1–$H1_{N1}$···O1A and O1A-$H1A_{O1A}$···N3, forming a six-membered N_3H_2O cycle. Due to these hydrogen bridges strand-like structures are formed in the crystalline state.

Molecular structure and atom labeling scheme of the formamidine (*syn-E*)-4-(EtOOC)-2-BrC_6H_3–N═CH–N(H)-Ph (**5**) are depicted in Fig. 4. The isoelectronic substitution of the central N atom by a CH fragment leads to a significant widening of the NEN bond angle. As characteristic for amidines [24], dimerization *via* N1–$H1_{N1}$···N2A hydrogen bridges occurs in the solid state leading to a centrosymmetric aggregate with an eight-membered

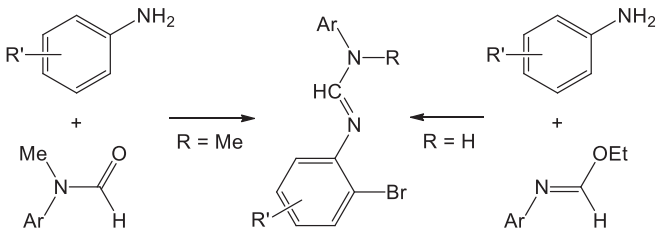

Scheme 8. Synthesis of asymmetric 1,3-diarylformamidines (R = H, right) and 1,3-diaryl-3-methylformamidines (R = Me, left).

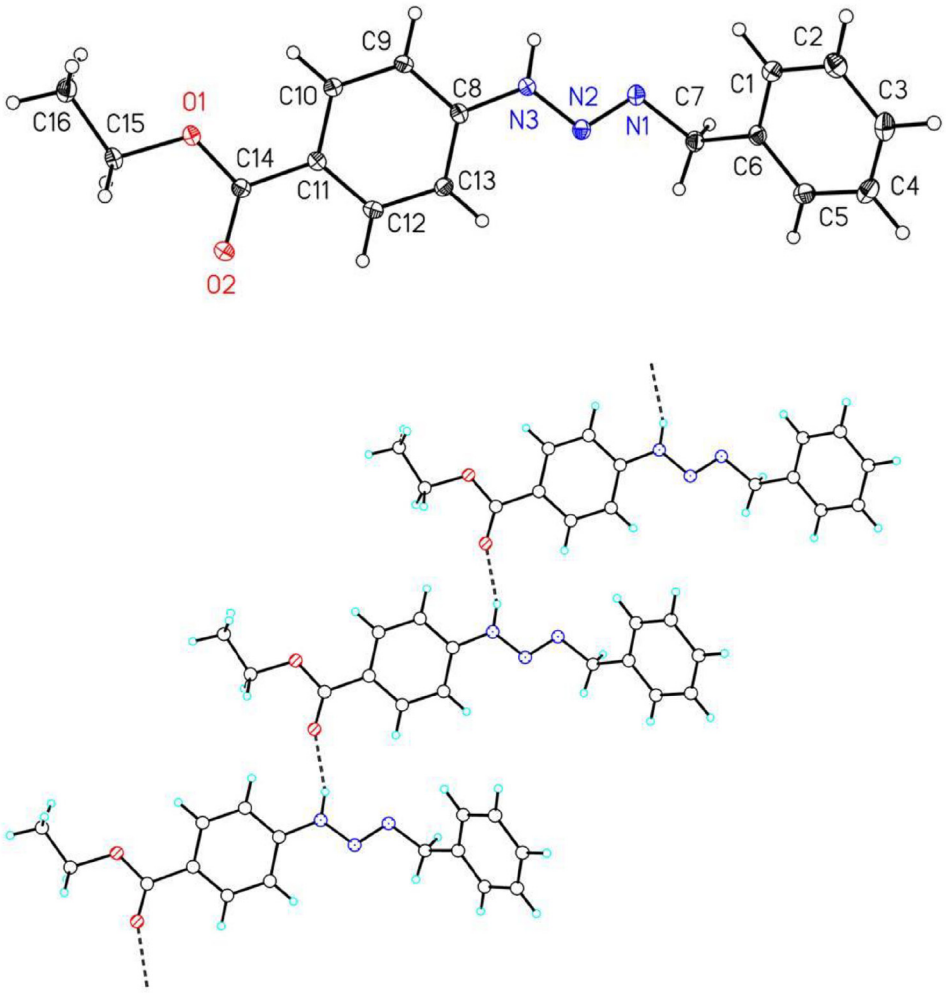

Fig. 2. Molecular structure and atom labeling scheme of (syn-E)-$PhCH_2$-N═N–N(H)–C_6H_4-4-COOEt (**3**) (top). The ellipsoids represent a probability of 30%, H atoms are shown with arbitrary radii. At the bottom, aggregation to a strand-like structure via N–H···O hydrogen bridges is depicted; the hydrogen bridges are shown with dotted lines.

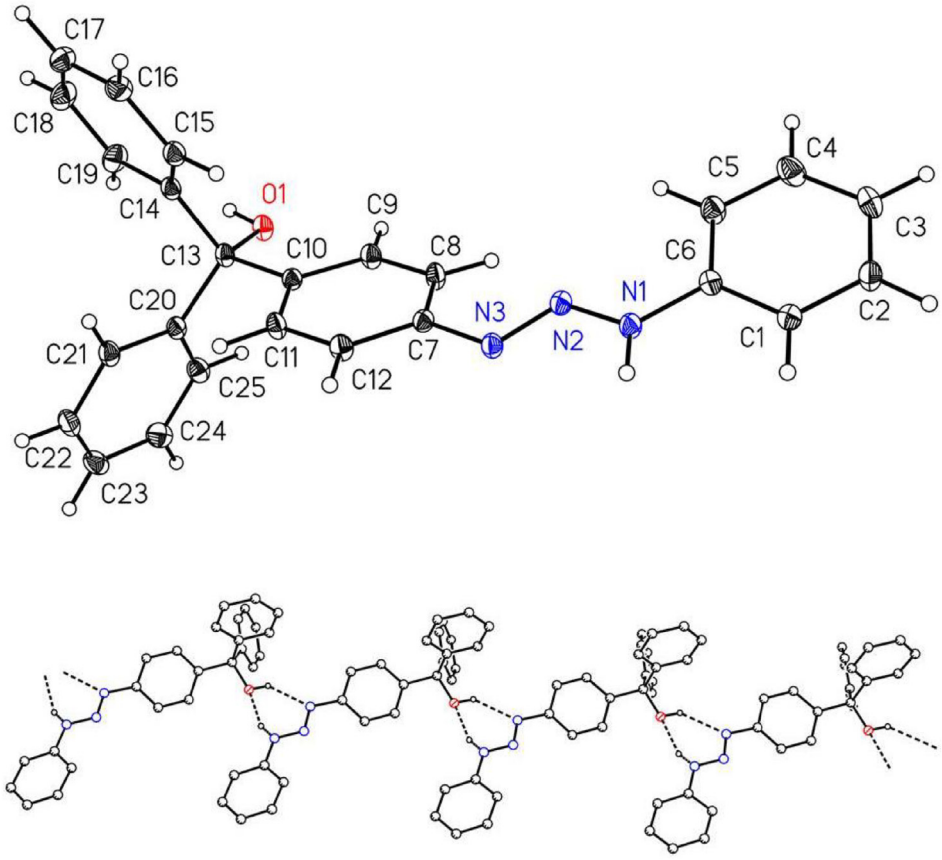

Fig. 3. Molecular structure and atom labeling scheme of (syn-E)-4-[Ph_2(HO)C−C_6H_4-]N═N−N(H)-Ph (**25**) (top). The ellipsoids represent a probability of 30%, H atoms are drawn with arbitrary radii. At the bottom, aggregation to a strand-like structure via N−H···O hydrogen bridges is depicted; the hydrogen bridges are shown with dotted lines.

(N2−C7−N1−$H1_{N1}$)$_2$ cycle. Despite the fact that the aryl group with the bromo substituent in *ortho*-position is oriented nearly perpendicular to the diazaallyl fragment due to steric reasons, the N1−C6 and N2−C8 bond lengths are very similar.

We included amidine derivatives with phenyl (benzamidines) and *tert*-butyl groups (pivalamidines) in 2-position of the 1,3-diazaallyl systems. This substitution pattern destabilizes the (*syn-E*)-isomeric form and the (*anti-E*)- (E = C-Ph) and (*syn-Z*)-configuration isomers (E = C-*t*Bu) [15] were observed. In these isomers dimerization *via* N−H···N hydrogen bridges is impossible. The structural motif of *(anti-E)-4*-(EtOOC)-2-BrC_6H_3−N═C(Ph)−N(H)−Ph (**7**) is shown in Fig. 5, molecular structure and atom labeling scheme of *(syn-Z)-4*-(EtOOC)-2-BrC_6H_3−N═C (*t*Bu)−N(H)−Ph (**8**) have been reported elsewhere [15]. The N−C bond lengths of the 1,3-diazaallyl moiety of **8** are comparable to compound **5** but the N−C−N bond angle is significantly widened to nearly 127.8 (3)° (**5**: 122.3 (4)°). Due to steric reasons compound **7** forms N1A-H1A···N2′ hydrogen bridges, leading to a strand-like aggregate. Contrary to this aggregation behavior, *(syn-Z)-4*-(EtOOC)-2-BrC_6H_3−N═C (*t*Bu)−N(H)−Ph (**8**) forms intermolecular N1−H1···O1′ hydrogen bridges, also leading to the formation of a one-dimensional aggregation polymer.

N-Methyl substitution prevents aggregation in the crystalline state and molecular structures were observed in solution and the solid. Despite the lack of hydrogen bridges as found in *NH*-triazenes, the structural parameters of *(syn-E)-4*-(EtOOC)C_6H_3−N═N−N (Me)-Ph (**9**) and (*syn-E*)-4-F-2-BrC_6H_3−N═N−N (Me)-Ph (**14**) are very similar. Molecular structure and atom labeling scheme of **9** are depicted in Fig. 6, those of *(syn-E)-4*-BrC_6H_4−N═N−N (Me)−C_6H_4-4-COOEt (**11**), containing two functionalized aryl groups, are shown in Fig. 7. Molecular structure and atom labeling scheme of (*syn-E*)-4-F-2-BrC_6H_3−N═N−N (Me)-Ph (**14**) are represented in the ESI.

The molecular structures of (*syn-E*)-4-F-2-BrC_6H_3−N═N−N (Me)-Ph (**14**), (*syn-E*)-4-Cl-2-BrC_6H_3−N═CH−N (Me)-Ph (**20**), and (*syn-E*)-2,4-$Br_2C_6H_3$−N═CH−N (Me)-Ph (**21**) are very similar. Therefore, only the molecular structure and atom labeling scheme of compound **20** is shown in Fig. 8, the structure of derivative **21** is depicted in the ESI. Additional *N*-methyl substitution of the triazenes leads to a slight widening of the NNN bond angles, whereas N-methylation of the formamidines does not affect the central NCN bond angle.

Selected structural parameters of triazenes and formamidines as well as *N*-methylated congeners are summarized in Table 2. Due to the fact that the number of asymmetrically *N,N′*-diaryl-substituted derivatives is quite small, we included selected symmetric 1,3-diaryltriazenes and -formamidines for comparison reasons. All triazenes and formamidines crystallized as (*syn-E*)-isomers regardless of the presence of methyl substituents at the formamidine (**5**, **20**, and **21**) and triazene moieties (**3** and **9**–**14**). Larger substituents like phenyl (**7**, benzamidinate) or *tert*-butyl groups (**8**, pivalamidinate) at the carbon atom of the NCN fragment enforce the (*anti-E*)- and (*syn-Z*)-isomeric forms, respectively. The (*syn-Z*)-isomeric form of the pivalamidine leads to a significant

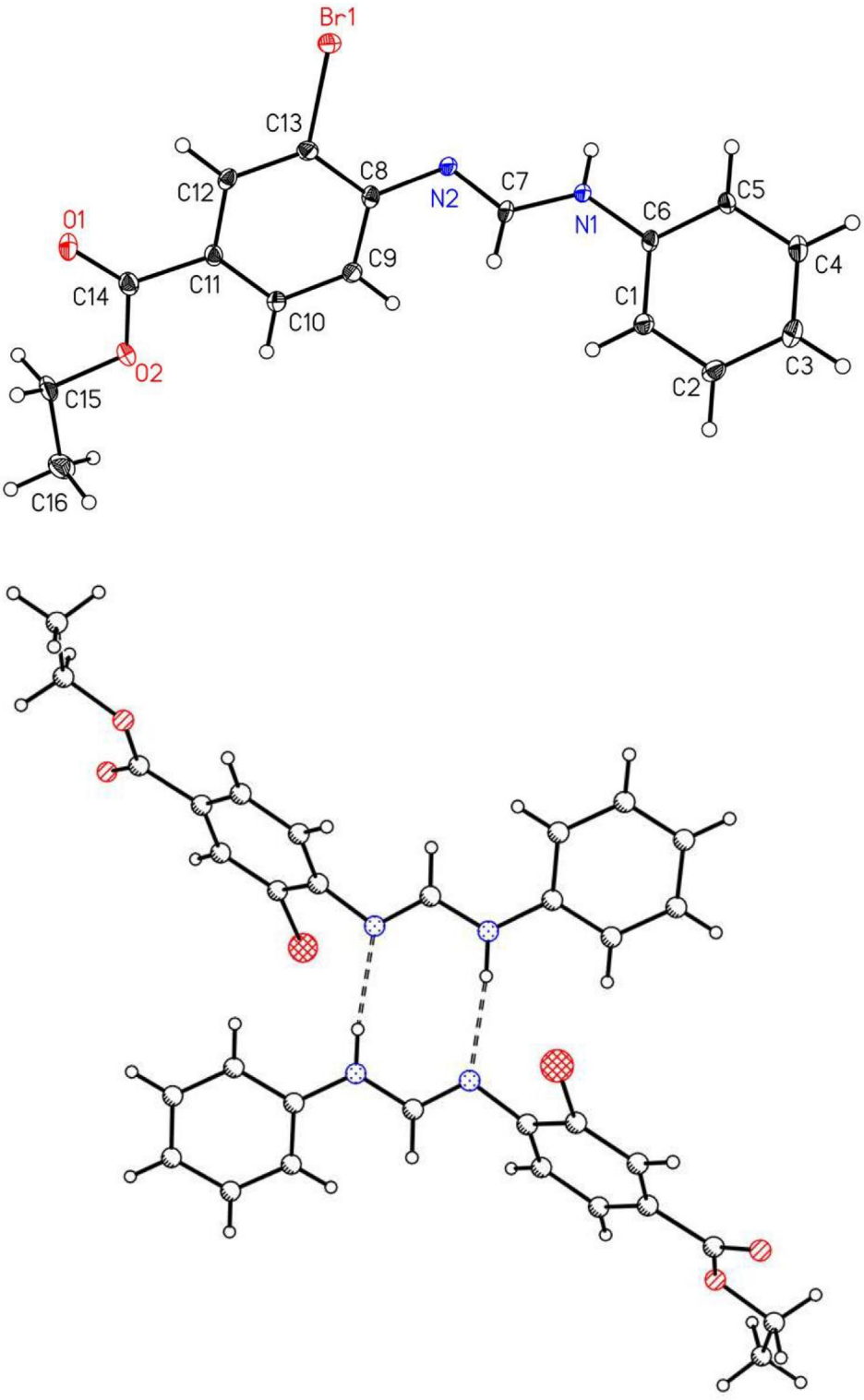

Fig. 4. Molecular structure and atom labeling scheme of (syn-E)-4-(EtOOC)-2-BrC_6H_3–N=CH–N(H)-Ph (**5**) (top). The ellipsoids represent a probability of 30%, H atoms are drawn with arbitrary radii. At the bottom, aggregation to dimeric units via N–H···N hydrogen bridges is depicted; the hydrogen bridges are shown with dotted lines.

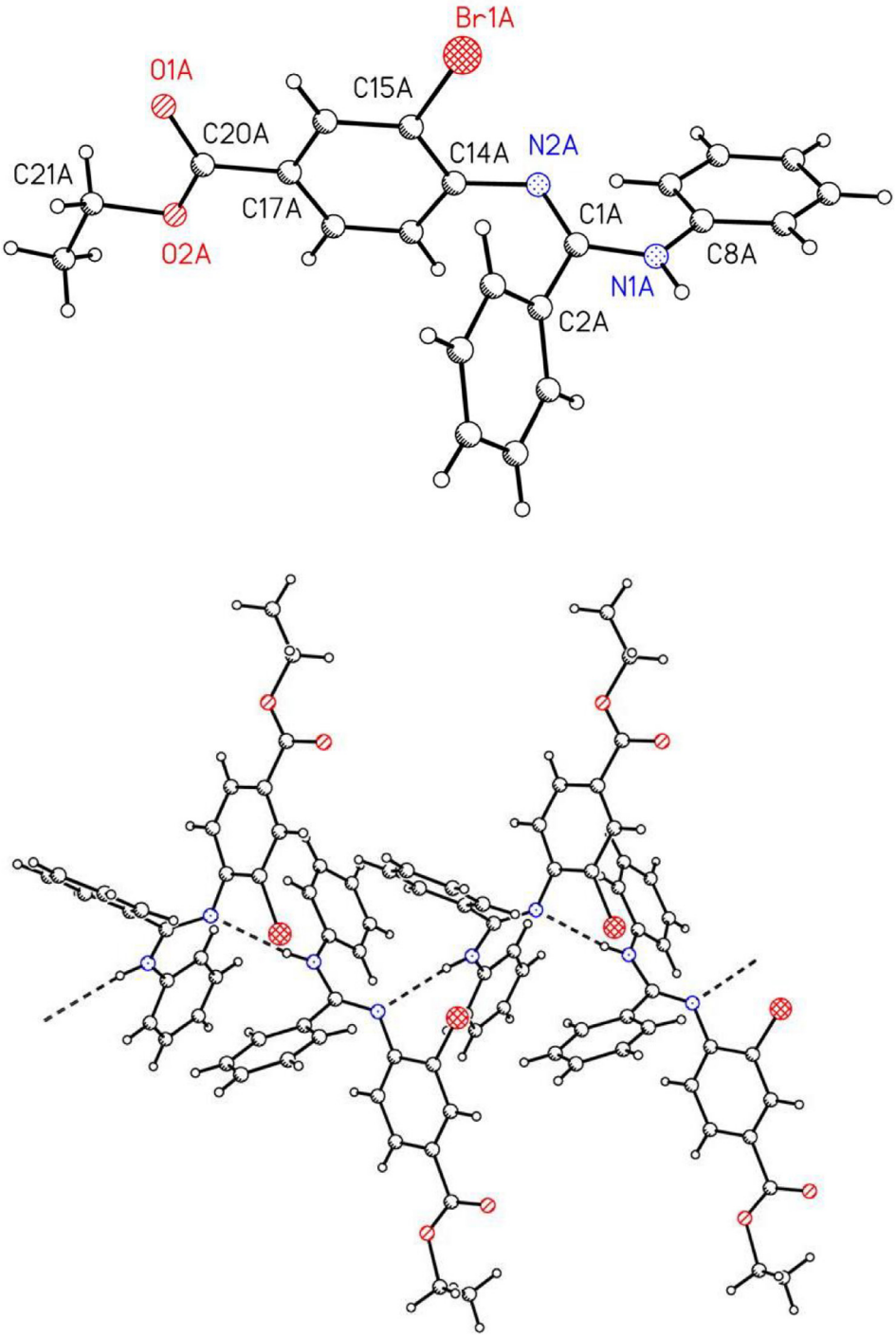

Fig. 5. Structural motif of (anti-E)-4-(EtOOC)-2-BrC_6H_3–N=C(Ph)–N(H)–Ph (**7**) (top). The atoms are drawn with arbitrary radii, all C-bound H atoms are omitted for clarity reason. At the bottom, aggregation to a strand structure is depicted; the hydrogen bridges are shown with dotted lines.

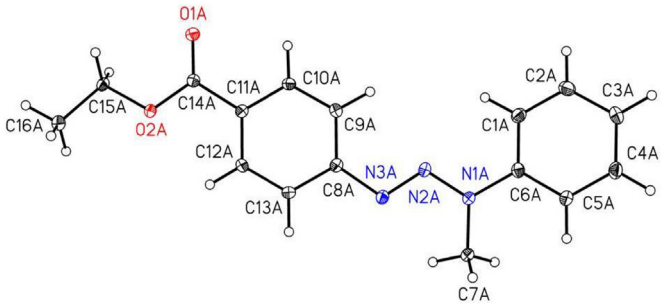

Fig. 6. Molecular structure and atom labeling scheme of molecule A of (syn-E)-4-(EtOOC)C_6H_3–N=CH–N (Me)-Ph (**9**). The ellipsoids represent a probability of 30%, H atoms are drawn with arbitrary radii.

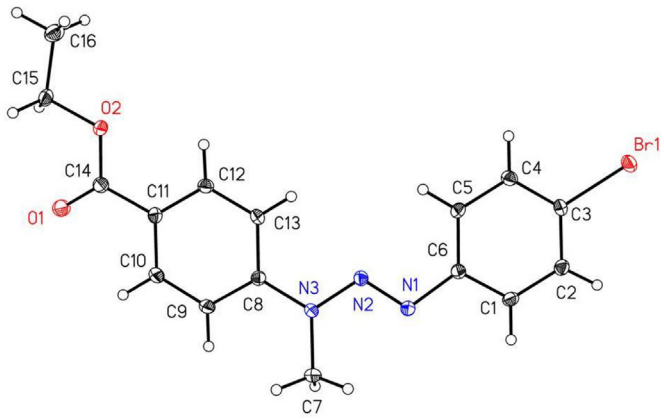

Fig. 7. Molecular structure and atom labeling scheme of (syn-E)-4-(EtOOC)-2-BrC_6H_3–N=CH–N (Me)-Ph (**11**). The ellipsoids represent a probability of 30%, H atoms are drawn with arbitrary radii.

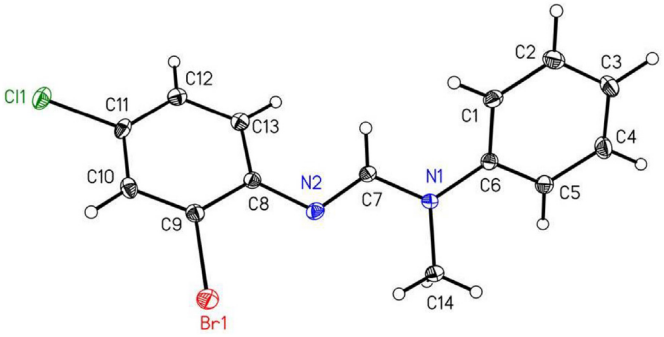

Fig. 8. Molecular structure and atom labeling scheme of (syn-E)-4-Cl-2-BrC_6H_3–N=CH–N (Me)-Ph (**20**). The ellipsoids represent a probability of 30%, H atoms are drawn with arbitrary radii.

widening of the NCN bond angle due to intramolecular steric repulsion between the aryl groups. Very bulky groups at the *N*-atom can also enforce different isomers as has been shown for 1,3-diaryl-3-triphenylmethyl-formamidine [31].

In 1,3-diarylformamidines and 1,3-diaryl-3-methylformamidines the NCN bond angles are slightly larger than 120°, a typical value for sp^2 hybridized carbon atoms. This value allows a straightforward dimerization *via* two collinear N–H···N hydrogen bridges. The contraction of the NEN bond angle to approx. 113° as found in the 1,3-diaryltriazenes and 1,3-diaryl-3-methyltriazenes destabilizes this kind of aggregation and other Lewis bases are advantageous for the formation of intermolecular hydrogen bridges, leading to strand-like aggregates.

In all these compounds the N = E double bonds are roughly 4–9 pm shorter than the E-N single bonds. Nearly ideal delocalization and very similar E = N and E-N bonds have been observed for the symmetric triazene 2-(MeOOC)C_6H_4–N=N–NH–C_6H_4-2-COOMe [25] and the symmetric formamidine F_5C_6–N=CH–NH–C_6F_5 [29]. In general, intramolecular steric strain influences configuration and conformation but the bond lengths are barely affected. Thus, the N–C_{Me} bond lengths to the methyl groups of approx. 146 pm are very similar for all compounds regardless of the nature of E (N, CH). The N-C_{aryl} distances to the aryl substituents vary between 139 and 143 p.m. In comparison to these values the NEN moieties with bond lengths around 127–130 pm for E = N double bonds and around 133–136 pm for E-N single bonds show slight charge delocalization leading to smaller differences than expected.

Palladium-mediated demethylating cyclohydroamination of *(syn-E)-4*-(EtOOC)-2-BrC_6H_3–N=N–N (Me)-Ph (**11**) yields the corresponding *N*-(4-ethoxycarbonyl)phenyl-benzotriazole (**26**, Scheme 2, left, R' = 4-COOEt) [12c]. Its molecular structure and numbering scheme are depicted in Fig. 9. The cyclization leads to a more acute NNN bond angle of 109.2 (2)° and slightly elongated N=N and N–N bonds with values of 129.9 (2) and 137.7 (2) pm, respectively. Nevertheless, these parameters correspond quite well to those of the unstrained triazenes, explaining the straightforward palladium-catalyzed formation of the triazole heterocycle. In contrast to this triazene cyclization, formamidines show no related reactivity pattern.

4. Conclusion

Asymmetric 1,3-diarylformamidines (E = CH) and -triazenes (E = N) as well as asymmetrically substituted 1,3-diaryl-3-methylformamidines and -triazenes of the type Ar'-N = E-N(R)-Ar (R = H, Me) represent important substance classes for the synthesis of azaheterocycles of biochemical and medicinal importance. Despite this application there are only very few structurally authenticated asymmetric derivatives known. The syntheses of these compounds is straightforward with moderate to excellent yields, making these compounds very attractive as substrates for e.g. Buchwald-Hartwig-type amination reactions and demethylating cycloamination for the preparation of substituted benzotriazoles. However, this protocol *via* diazotization of substituted aminobenzenes and reaction with arylamines is not suitable for the preparation of doubly triazenyl-functionalized benzene.

In the crystalline state, the studied formamidines and triazenes favor the (*syn-E*) configuration at the central NEN-fragments. Bulky groups at the central carbon atom (E = CH, formamidines) and/or at the nitrogen base introduce severe intramolecular strain which destabilizes this configuration and other isomers are preferred. In agreement with the chemical NMR shifts, the *N*-bound methyl groups show very similar bonding parameters regardless of the substitution pattern of the aryl groups and of the nature of E (amidines, triazenes).

In the solid state, 1,3-diarylformamidines dimerize *via* two nearly colinear N–H···N hydrogen bridges. This kind of aggregation is impossible for 1,3-diaryltriazenes due to a significantly narrower NEN bond angle of approx. 113° whereas the formamidines exhibit NCN values of around 122°. Due to this structural difference the investigated triazenes favor intermolecular N–H···O hydrogen bridges to oxygen bases, leading to strand-like aggregates (Table 3). Due to the fact that bulky groups enforce another isomeric form than (*syn-E*)-configuration, strand-like structures are formed *via* intermolecular N–H···N or N–H···O hydrogen bridges. These weak hydrogen bridges are highly asymmetric and quasi-linear with DHA

Table 2
Comparison of structural parameters (bond lengths (pm) and angles (deg.)) of selected 1,3-diaryltriazenes (R = H) and 1,3-diaryl-3-methyltriazenes (R = Me) of the type Ar–N=N–N(R)-R′ as well as of 1,3-diarylamidines (R = H) and 1,3-diaryl-3-methylamidines (R = Me).[a]

	Isomer	E	R	Ar	R′	N-C_{Ar}	N = E	E-N	N-$C_{R'}$	N–C_{Me}	NEN	Ref.
3	*Syn-E*	N	H	C_6H_4-2-COOMe	C_6H_4-2-COOMe	141.8 (3)	129.6 (3)	129.3 (3)	140.9 (3)	–	113.6 (2)	[25]
	Syn-E	N	H	C_6H_3-2,4-Br_2	C_6H_3-2,4-Br_2	142.2 (7)	126.7 (7)	133.2 (7)	138.8 (8)	–	111.6 (5)	[26]
	Syn-E	N	H	C_6H_4-2-Cl	C_6H_4-2-OEt	141.7 (3)	126.3 (3)	132.8 (3)	139.7 (3)	–	112.9 (2)	[27]
	Syn-E	N	H	C_6H_4-4-Cl	C_6H_4-2-OMe	141.5 (2)	125.9 (2)	133.0 (2)	139.0 (2)	–	111.4 (1)	[28]
	Syn-E	N	H	CH_2-Ph	C_6H_4-4-COOEt	146.9 (2)	125.9 (2)	134.9 (2)	139.0 (2)	–	111.5 (1)	Here
25	*Syn-E*	N	H	C_6H_4–$C(Ph)_2OH$	Ph	142.9 (2)	128.3 (2)	132.1 (2)	141.1 (2)	–	113.9 (1)	Here
5	*Syn-E*	CH	H	C_6H_4-3-Br	C_6H_4-3-Br	141.0 (8)	129.6 (8)	135.6 (8)	139.4 (8)	–	122.4 (6)	[24]
	Syn-E	CH	H	C_6H_4-4-F	C_6H_4-4-F	141.8 (2)	128.3 (3)	134.2 (2)	141.4 (2)	–	122.2 (2)	[24]
	Syn-E	CH	H	C_6H_3-2,6-F_2	C_6H_3-2,6-F_2	140.9	128.6	134.4	140.6	–	120.5	[29]
	Syn-E	CH	H	C_6H_2-2,3,5-F_3	C_6H_2-2,3,5-F_3	141.0	129.8	133.1	139.6	–	122.2	[29]
	Syn-E	CH	H	C_6H_2-3,4,5-F_3	C_6H_2-3,4,5-F_3	142.2	128.0	135.1	140.1	–	121.8	[29]
	Syn-E	CH	H	C_6F_5	C_6F_5	141.2	131.1	133.1	140.1	–	121.0	[29]
	Syn-E	CH	H	C_6H_3-2-Br-4-COOEt	Ph	141.1 (5)	128.5 (5)	135.5 (5)	135.5 (5)	–	122.3 (4)	Here
7	*Anti-E*	C-Ph	H	C_6H_3-2-Br-4-COOEt	Ph	141.9 (13)	130.5 (12)	136.3 (13)	139.7 (13)	–	121.4 (9)	Here
8	*Syn-Z*	C-*t*Bu	H	C_6H_3-2-Br-4-COOEt	Ph	138.1 (4)	128.0 (4)	136.4 (4)	142.2 (4)	–	127.9 (3)	[15]
9	*Syn-E*	N	Me	C_6H_4-4-COOEt	Ph	141.8 (2)	127.5 (2)	133.1 (2)	142.2 (2)	145.9 (2)	113.9 (1)	Here
11	*Syn-E*	N	Me	C_6H_4-4-Br	C_6H_4-4-COOEt	142.8 (2)	127.0 (2)	134.0 (2)	141.6 (2)	145.8 (2)	114.5 (2)	Here
12	*Syn-E*	N	Me	C_6H_3-2-Br-4-COOEt	Ph	141.1 (4)	128.1 (3)	132.5 (3)	141.9 (3)	146.6 (4)	113.3 (2)	[30]
14	*Syn-E*	N	Me	C_6H_3-2-Br-4-F	Ph	142.2 (3)	127.3 (2)	134.4 (2)	141.8 (2)	146.2 (3)	113.3 (2)	Here
20	*Syn-E*	CH	Alkyl[b]	C_6H_3-2,6-*i*Pr_2	C_6H_3-2,6-*i*Pr_2	141.8 (4)	128.2 (4)	136.1 (4)	145.1 (4)	146.5 (4)	122.3 (3)	[31]
	Anti-E	CH	CPh_3	C_6H_3-2,6-Me_2	C_6H_3-2,6-Me_2	140.4	128.1	136.8	142.3	150.9	122.3	[32]
	Syn-E	CH	Me	C_6H_2-2,4,6-Me_3	Ph	143.0 (3)	126.8 (3)	136.3 (3)	141.7 (3)	146.8 (3)	123.5 (3)	[33]
	Syn-E	CH	Me	C_6H_3-2-Br-4-Cl	Ph	139.7 (4)	128.1 (4)	136.0 (6)	142.1 (4)	146.1 (4)	121.0 (3)	Here
21	*Syn-E*	CH	Me	C_6H_3-2,4-Br_2	Ph	139.6 (3)	128.6 (3)	135.3 (3)	141.9 (3)	146.4 (3)	121.1 (2)	Here

[a] Data without estimated standard deviations were taken from the CSD data base.
[b] Alkyl $(CH_2)_4$–O–C_6H_2-3,4,5-F_3.

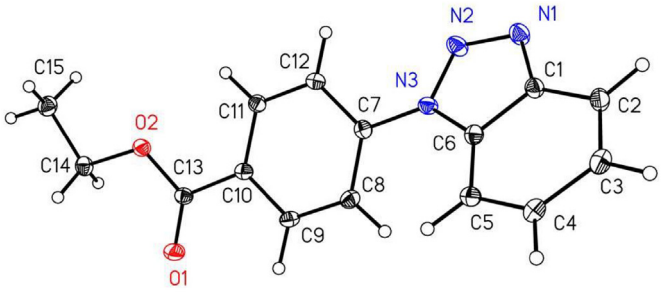

Fig. 9. Molecular structure and atom labeling scheme of N-(4-ethoxycarbonyl)phenyl-benzotriazole (**26**). The ellipsoids represent a probability of 30%, H atoms are drawn with arbitrary radii.

bond angles larger than 160°. In compound **7** the very large N1A/N1B···N2B'/N2A′ distances are characteristic for very weak hydrogen bridges caused by steric hindrance. The N1···N2' distance in unstrained derivative **5** is significantly smaller verifying a stronger hydrogen bridge-supported network.

Author contributions section

Silvio Preusser: Synthesis of triazenes and formamidines, data collection. Paul R. W. Schönherr: triazene syntheses, data collection. Helmar Görls: X-ray structure elucidation. Sven Krieck: data analysis, manuscript conception. Wolfgang Imhof: study conception, manuscript editing. Matthias Westerhausen: Supervision of scientific work, study conception, manuscript draft.

Declaration of interest

Amidines and triazenes are an important substance class to stabilize low valent metal complexes or to protect highly reactive bonds. Nevertheless, the protonated formes - amidines and triazenes - attracted significantly less attention. We studied these compounds in more detail because they show a significant difference in reactivity with respect to cyclization and formation of benzotriazole from triazenes whereas the formamidines do not undergo cyclization under similar reaction conditions.

This journal is prune to present and discuss structural features, similarities as well as significant differences.

Table 3
Intermolecular hydrogen bridges of the type D-H···A (distances (pm) and DHA bond angles (deg.)) leading to aggregation of 1,3-diaryltriazenes and 1,3-diarylamidines.

Comp.	D-H···A	Aggregate	D-H	H···A	D···A	DHA	Ref.
3	N3–$H3_{N3}$···O2′	Strand	89 (2)	200 (2)	285.7 (2)	160 (2)	
5	N1–$H1_{N1}$···N2′	Cyclic dimer	88	208	295.2 (5)	170	
7	N1A-$H1A_{N1A}$···N2B′	Strand	88	247	335 (1)	173	
	N1B–$H1B_{N1B}$···N2A′	Strand	88	254	341 (1)	172	
8	N1–$H1_{N1}$···O1′	Strand	74 (4)	218 (4)	290.8 (4)	167 (4)	[15]
24	N3–$H3_{N3}$···O1′	Strand	86 (5)	210 (5)	291.2 (5)	156 (5)	

Buchwald-Hartwig-type amination reactions and demethylating cycloamination of triazenes lead to benzotriazoles with a five-membered N_3C_2 cycle. A comparable reactivity has not been observed for related isoelectronic formamidines.

Acknowledgement

The work is based on industrial collaboration and we thank Laborchemie Apolda GmbH, Germany, for generous financial support. Advanced students supported these investigations in the frame of their inorganic and organometallic laboratory courses. We also acknowledge the valuable support of the NMR (www.nmr.uni-jena.de/) and mass spectrometry service platforms (www.ms.uni-jena.de/) of the Faculty of Chemistry and Earth Sciences of the Friedrich Schiller University Jena, Germany.

Appendix A. Supplementary data

Supplementary data to this article can be found online at https://doi.org/10.1016/j.molstruc.2019.127622.

References

[1] a) Z. Rappoport, S. Patai (Eds.), The Chemistry of Amidines and Imidates (Chemistry of Functional Groups), Wiley, Chichester, 1991;
b) T. Ishikawa (Ed.), Superbases for Organic Synthesis, Wiley, Chichester, 2009.
[2] a) T. Giraldi, T.A. Connors, G. Cartei (Eds.), Triazenes: Chemical, Biological, and Clinical Aspects, Plenum Press, New York, 1990;
b) S. Patil, A. Bugarin, Fifty years of π-conjugated triazenes, Eur. J. Org. Chem. (2016) 860–870.
[3] a) R.L. Shriner, F.W. Neumann, The chemistry of the amidines, Chem. Rev. 35 (1944) 351–425;
b) K. Vaughan, M.F.G. Stevens, Monoalkyltriazenes, *Chem. Soc. Rev*. 7 (1978) 377–397;
c) M.S. dos Santos, A.M.R. Bernardino, M.C. de Souza, Principal methods for synthesis of amidines, Quim. Nova 29 (2006) 1301–1306.
[4] a) A. Kreutzberger, Amidine structure in pharmaceutical research, *Progr*, Drug Res. 11 (1968) 356–445;
b) J.V. Greenhill, P. Lue, Amidines and guanidines in medicinal chemistry, Prog. Med. Chem. 30 (1993) 203–326;
c) R.A. Michelin, P. Sgarbossa, S.M. Sbovata, V. Gandin, C. Marzano, R. Bertani, Chemistry and biological activity of platinum amidine complexes, ChemMedChem 6 (2011) 1172–1183;
d) M.N.C. Soeiro, K. Werbovetz, D.W. Boykin, W.D. Wilson, M.Z. Wang, A. Hemphill, Novel amidines and analogues as promising agents against intracellular parasites: a systemic review, Parasitology 140 (2013) 929–951;
e) C. Maccallini, M. Fantacuzzi, R. Amoroso, Amidine-based bioactive compounds for the regulation of arginine metabolism, Mini Rev. Med. Chem. 13 (2013) 1305–1310;
f) G. Kantin, M. Krasavin, N-Arylation of amidines and guanidines: an update, Curr. Org. Chem. 20 (2016) 1370–1388;
g) N. Re, M. Fantacuzzi, C. Maccallini, R. Paciotti, R. Amoroso, Recent developments of amidine-like compounds as selective NOS in hibitors, Curr. Enzym. Inhib. 12 (2016) 30–39.
[5] a) M. Julliard, G. Vernin, Antitumor triazenes, Bull. Soc. Chim. Fr. (1981) 150–159;
b) A. Gescher, M.D. Threadgill, The metabolism of triazene antitumor drugs, Pharmacol. Ther. 32 (1987) 191–205;
c) D.E.V. Wilman, The development of a second-generation triazene, Cancer Treat Rev. 15 (1988) 69–72;
d) F. Marchesi, M. Turriziani, G. Tortorelli, G. Avvisati, F. Torino, L. de Vecchis, Triazene compounds: mechanism of action and related DNA repair systems, Pharmacol. Res. 56 (2007) 275–287;
e) L. Bonmassar, F. Marchesi, E. Pascale, O. Franzese, G.P. Margison, A. Bianchi, S. D'Atri, S. Bernardini, D. Lattuada, E. Bonmassar, Triazene compounds in the treatment of acute myeloid leukemia: a short review and a case report, Curr. Med. Chem. 20 (2013) 2389–2401.
[6] a) M. Tisler, Heterocyclic amidines and hydroxylamidines as synthons for bi- and polycyclic heterocycles, Heterocycles 20 (1983) 1591–1614;
b) A.A. Aly, A.M. Nour-El-Din, Functionality of amidines and amidrazones, ARKIVOC (1) (2008) 153–194;
c) S. Chiba, Copper-catalyzed oxidative molecular transformation of amidines for synthesis of nitrogen heterocycles, Tetrahedron Lett. 57 (2016) 3678–3683;
d) A.A. Aly, S. Bräse, M.A.-M. Gomaa, ARKIVOC (6) (2018) 85–138;
e) I.A. Perillo, M.C. Caterina, A. Salerno, ARKIVOC (1) (2018) 288–318.
[7] a) D.B. Kimball, M.M. Haley, Triazenes: a versatile tool in organic synthesis, Angew. Chem. Int. Ed. 41 (2002) 3338–3351;
b) S. Bräse, The virtue of the multifunctional triazene linkers in the efficient solid-phase synthesis of heterocycle libraries, Acc. Chem. Res. 37 (2004) 805–816;
c) D.K. Kölmel, N. Jung, S. Bräse, Azides – diazonium ions – triazenes: versatile nitrogen-rich functional groups, Aust. J. Chem. 67 (2014) 328–336;
d) Y. Zhang, D. Cao, W. Liu, H. Hu, X. Zhang, C. Liu, Recent applications of aryltriazenes in organic synthesis *via* C-N/N-N bond cleavage, Curr. Org. Chem. 19 (2015) 151–178.
[8] a) F.T. Edelmann, Lanthanide amidinates and guanidinates: from laboratory curiosities to efficient homogeneous catalysts and precursors for rare-earth oxide thin films, Chem. Soc. Rev. 38 (2009) 2253–2268;
b) F.T. Edelmann, Homogeneous catalysis using lanthanide amidinates and guanidinates, Struct. Bonding 137 (2010) 109–163;
c) S. Collins, Polymerization catalysis with transition metal amidinate and related complexes, Coord. Chem. Rev. 255 (2011) 118–138;
d) J.E. Taylor, S.D. Bull, J.M.J. Williams, Amidines, isothioureas, and guanidines as nucleophilic catalysts, Chem. Soc. Rev. 41 (2012) 2109–2121;
e) T.R.M. Rauws, B.U.W. Maes, Transition metal-catalyzed N-arylations of amidines and guanidines, Chem. Soc. Rev. 41 (2012) 2463–2497;
f) F.T. Edelmann, Lanthanide amidinates and guanidinates in catalysis and materials science: a continuing success story, Chem. Soc. Rev. 41 (2012) 7657–7672;
g) J.Y. Quek, T.P. Davis, A.B. Lowe, Amidine functionality as a stimulus-responsive building block, Chem. Soc. Rev. 42 (2013) 7326–7334.
[9] Z. Li, Q. Zhang, J. Pan, Recent advances with regard to triazene derivatives as chromogenic reagents in analytical chemistry, Rev. Anal. Chem. 22 (2003) 191–232.
[10] a) J. Barker, M. Kilner, The coordination chemistry of the amidine ligand, Coord. Chem. Rev. 133 (1994) 219–300;
b) M.P. Coles, Application of neutral amidines and guanidines in coordination chemistry, Dalton Trans. (2006) 985–1001;
c) D.A. Kissounko, M.V. Zabalov, G.P. Brusova, D.A. Lemenovskii, Principal trends in the chemistry of amidinate complexes of main-group and transition elements, Russ. Chem. Rev. 75 (2006) 351–374;
d) F.T. Edelmann, Advances in the coordination chemistry of amidinate and guanidinate ligands, Adv. Organomet. Chem. 57 (2008) 183–352.
[11] Q.-L. Liu, D.-D. Wen, C.-C. Hang, Q.-L. Li, Y.-M. Zhu, A novel and regiospecific synthesis of 1-aryl-1*H*-benzotriazoles *via* copper(I)-catalyzed intramolecular cyclization reaction, Helv. Chim. Acta 93 (2010) 1350–1354. For recent reviews on Buchwald-Hartwig-type reactions see:;
a) G. Evano, N. Blanchard, M. Toumi, Copper-mediated coupling reactions and their applications in natural products and designed biomolecules synthesis, Chem. Rev. 108 (2008) 3054–3131;
b) P. Ruiz-Castillo, S.L. Buchwald, Applications of palladium-catalyzed C-N cross-coupling reactions, Chem. Rev. 116 (2016) 12564–12649;
c) M.M. Heravi, Z. Kheilkordi, V. Zadsirjan, M. Heydari, M. Malmir, Buchwald-Hartwig reaction: an overview, J. Organomet. Chem. 861 (2018) 17–104.
[12] a) J. Zhou, J. He, B. Wang, W. Yang, H. Ren, 1,7-Palladium migration *via* C-H activation, followed by intramolecular amination: regioselective synthesis of benzotriazoles, J. Am. Chem. Soc. 133 (2011) 6868–6870;
b) R.K. Kumar, M.A. Ali, T. Punniyamurthy, Org. Lett. 13 (2011) 2102–2105;
c) K. Takagi, M. Al-Amin, N. Hoshiya, J. Wouters, H. Sugimoto, Y. Shiro, H. Fukuda, S. Shuto, M. Arisawa, Palladium-nanoparticle-catalyzed 1,7-palladium migration involving C-H activation, followed by intramolecular amination: regioselective synthesis of *N*1-arylbenzotriazoles and an evaluation of their inhibitory activity toward indoleamine 2,3-dioxygenase, J. Org. Chem. 79 (2014) 6366–6371.
[13] R.M. Roberts, T.D. Higgins, P.R. Noyes, Ortho esters, imidic esters and amidines. VI. Two general methods of synthesis of N-phenylformimidic esters involving transesterification, J. Am. Chem. Soc. 77 (1955) 3801–3805.
[14] D. Li, N. Xu, Y. Zhang, L. Wang, A highly efficient Pd-catalyzed decarboxylative ortho-arylation of amides with aryl acylperoxides, Chem. Commun. 50 (2014) 14862–14865.
[15] S. Preusser, D. Kalden, D. Bevern, A. Oberheide, H. Görls, W. Imhof, M. Westerhausen, S. Krieck, Potassium salts of asymmetrically substituted amidinates and a triazenide, Eur. J. Inorg. Chem. (2019) 1970–1978.
[16] R. Hooft, COLLECT, Data Collection Software, Nonius B.V., Netherlands, 1998.
[17] inZ. Otwinowski, W. Minor (Eds.), in: C.W. Carter, R.M. Sweet (Eds.), Methods in Enzymology, vol. *276*, Academic Press, New York, 1997, pp. 307–326. Macromolecular Crystallography, Part A.
[18] SADABS 2.10, Bruker-AXS inc., Madison, WI, USA, 2002.
[19] G.M. Sheldrick, A short history of SHELX, Acta Crystallogr. A64 (2008) 112–122.
[20] G.M. Sheldrick, Crystal structure refinement with SHELXL, Acta Crystallogr. C71 (2015) 3–8.
[21] A.L. Spek, Platon squeeze: a tool for the calculation of the disordered solvent contribution to the calculated structure factors, Acta Crystallogr. C**71** (2015) 9–18.
[22] XP, Siemens Analytical X-Ray Instruments Inc., Karlsruhe, Germany, 1990, 1994. Madison, WI, USA.
[23] A.A. Durgaryan, R.A. Arakelyan, N.A. Durgaryan, E.E. Matinyan, Synthesis and study of a polymer containing di- and triazenyl-*p*-phenylene groups, Russ. J. Gen. Chem. 84 (2014) 860–864.
[24] R. Anulewicz, I. Wawer, T.M. Krygowski, F. Männle, H.-H. Limbach, Combined X-ray diffraction and ^{15}N CPMAS NMR study of molecular structure and proton order/disorder phenomena in cyclic *N,N'*-bisarylformamidine dimers, J. Am. Chem. Soc. 119 (1997) 12223–12230.
[25] J.G. Rodríguez, M. Parra-Hake, G. Aguirre, F. Ortega, P.J. Walsh, Synthesis and structure of a dinuclear copper complex of a bis(bidentate)triazenide ligand, Polyhedron 18 (1999) 3051–3055.
[26] M. Hörner, I.C. Casagrande, J. Bordinhao, C. Mössmer, 1,3-Bis(2,4-

dibromophenyl)triazene, Acta Crystallogr. C58 (2002) o193–o194.
[27] M.K. Rofouei, J.A. Gharamaleki, M.R. Melardi, S.M. Hosseini, F. Hosseinzadeh, M. Peyman, A. Ghannadan, B. Notash, G. Bruno, H.A. Rudbari, Synthesis, characterization and crystal structures of Hg^{II} complexes with asymmetric ortho-functionalized 1,3-bis(aryl)triazenide ligands, Polyhedron 44 (2012) 138–142.
[28] M.K. Rofouei, Z. Ghalami, J.A. Gharamaleki, V. Ghoulipour, G. Bruno, H.A. Rudbari, Synthesis, structure, and solution study of a mercury(II) complex with the ligand [1-(2-methoxyphenyl)-3-(4-chlorophenyl)]triazene, Z. Anorg. Allg. Chem. 638 (2012) 798–803.
[29] S. Krackl, S. Inoue, M. Driess, S. Enthaler, Intermolecular hydrogen-fluorine interaction in dimolybdenum triply bonded complexes modified by fluorinated formamidine ligands for the construction of 2D- and 3D-networks, Eur. J. Inorg. Chem. (2011) 2103–2111.
[30] S. Preusser, P. Schönherr, H. Görls, W. Imhof, S. Krieck, M. Westerhausen, Palladium(II) complexes derived from 1-(2-bromo-4-ethoxycarbonylphenyl)-3-phenyltriazenes, J. Organomet. Chem. 898 (2019), https://doi.org/10.1016/j.jorganchem.2019.120875 online.
[31] M.L. Cole, G.B. Deacon, C.M. Forsyth, P.C. Junk, K. Konstas, J. Wang, Steric modulation of coordination number and reactivity in the synthesis of lanthanoid(III) formamidinates, Chem. Eur J. 13 (2007) 8092–8110.
[32] D. Werner, G.B. Deacon, P.C. Junk, R. Anwander, Cerium(III/IV) formamidinate chemistry, and a stable cerium(IV) diolate, Chem. Eur J. 20 (2014) 4426–4438.
[33] S. Enthaler, K. Schröder, S. Inoue, B. Eckhardt, K. Junge, M. Beller, M. Drieß, Formamidines – versatile ligands for zinc-catalyzed hydrosilylation and iron-catalyzed epoxidation reactions, Eur. J. Inorg. Chem. (2010) 4893–4901.